



# Computational fluid dynamics (CFD) modelling and experimental validation of thermal processing of canned fruit salad in glass jar



Matteo Cordioli <sup>a</sup>, Massimiliano Rinaldi <sup>a</sup>, Gabriele Copelli <sup>b</sup>, Paolo Casoli <sup>b</sup>, Davide Barbanti <sup>a,\*</sup>

<sup>a</sup> Department of Food Science, University of Parma, Parco Area delle Scienze 47/A, 43124 Parma, Italy

<sup>b</sup> Department of Industrial Engineering, University of Parma, Parco Area delle Scienze 181/A, 43124 Parma, Italy

## ARTICLE INFO

### Article history:

Received 5 March 2014

Received in revised form 29 October 2014

Accepted 2 November 2014

Available online 15 November 2014

### Keywords:

CFD

Thermal processing

Canned fruit salad

Natural convection

Conduction

## ABSTRACT

In this paper the heat transfer of a fruit salad during the pasteurization treatment was investigated. The objective of the paper was to develop and validate a computational fluid dynamics (CFD) model for predicting the temperature profiles during the thermal processing of this sample. Samples of a commercial fruit salad, composed of five different fruits with different shapes, sizes and thermal properties, submerged in water/sugar syrup, were submitted to thermal treatments in a pilot plant and temperature profiles at different locations were experimentally recorded. Results showed that the slowest heating point (SHP) was positioned at 19–20% of the can height: fruit closest to the SHP such as pear presented the lowest *F* value. Moreover, *F* values resulted to be influenced by the distance from the jar bottom as function of natural convection motion of the syrup. CFD model simulations data were then successfully validated against the experimental ones: results, expressed as RMSE, showed a good fitting between calculated and experimental data, both for syrup (mean RMSE 1.47 °C) and fruit pieces (mean RMSE 1.63 °C). In addition, *F* values calculated from both experimental and simulated temperatures resulted very similar with only little differences. In conclusion, the proposed approach and mathematical model can thus be usefully applied for the simulation and prediction of thermal processes of canned fruit salad for process design and optimization.

© 2014 Elsevier Ltd. All rights reserved.

## 1. Introduction

In the food industry, a great number of fruits and vegetables are packaged in cans or jars, filled with an appropriate sugar syrup or brine, and thermally processed in order to increase their shelf life through the inactivation of both spoilage microorganisms and enzymes (Kiziktas et al., 2010).

Heat transfer mechanisms in canned food are conduction for solid and high viscosity liquid foods, natural convection for low viscosity liquid foods, convection plus conduction for liquid foods with solid particles and convection followed by conduction for liquid foods containing starch or viscosity modifiers (Chen and Ramaswamy, 2007).

Moreover, it is widely known that quality as well as nutritional characteristics of foods can be dramatically reduced by the thermal stabilisation processes. Hence, time and temperature combination during the heating and the cooling cycles must be properly assessed to guarantee both effectiveness (inactivation of microorganisms and enzymes) and efficiency (retention of sensory and

nutritional characteristics as well as limiting of costs). As a consequence, the thermal process must be properly designed by studying the thermal properties of foods and the mechanism of heat transfer during the treatment. These purposes are normally achieved by a relevant number of experimental trials with an increase in costs and time consumption thus reducing the possibility to have fast, efficient and in-depth results (Sun, 2007).

In order to overcome these limits, in the last years, process design in the food industry has been increasingly carried out by using numerical solutions of process governing equations, modelling and calculation methods (Weng, 2005).

Among these, computational fluid dynamics (CFD), has found widespread application in many areas of food processing such as spray drying, baking, sterilization, heat exchangers design, chilling, mixing, fermentation and in the agri-food industry (Sun, 2007).

CFD is a simulation tool which uses powerful computers and applied mathematics to model fluid flow situations for the prediction of heat, mass, momentum transfer and optimal design in industrial processes (Anandharamakrishnan, 2011; Chhanwal et al., 2012; Kuriakose and Anandharamakrishnan, 2010; Xia and Sun, 2002). Several works deal with CFD simulations of canned foods: Kumar et al. (1990) simulated the natural convection in

\* Corresponding author. Tel.: +39 521 905706.

E-mail address: [davide.barbanti@unipr.it](mailto:davide.barbanti@unipr.it) (D. Barbanti).

canned thick viscous liquid foods; Ghani et al. (1999, 2002) studied the natural convection heating of canned foods in vertical and horizontal positions, showing faster heating in the vertical can, which is expected due to the enhancement of natural convection caused by its greater height. The effect of the inclination of container walls and geometry modification on the sterilization process was also investigated by Varma and Kannan (2005).

A few works have been published on the CFD simulation studies of canned foods with solid/liquid mixture. These include heat transfer and liquid flow prediction during the sterilization of large particles in a cylindrical vertical can (Rabiey et al., 2007) and the heat transfer in canned peas under pasteurization (Kiziktas et al., 2010). Ghani and Farid (2006) analysed and successfully modelled the thermal sterilization process of canned solid–liquid food mixture (pineapple slices with governing liquid) in metal cans, indicating that natural convection effects in the liquid played a significant role in the evolution of temperature. In the same way, Dimou and Yanniotis (2011) studied the temperature profile, the velocity profile and the slowest heating zone in a still can filled with food items with cylindrical–conical shape such as asparagus. With regard to pineapples, Padmavati and Anandharamakrishnan (2013) investigated the effect of size reduction of the product (pineapple slices vs. tidbits) on the effectiveness of heat transfer during thermal processing.

However, the scientific literature still lacks a comprehensive simulation study for the prediction of temperature changes of solid–liquid mixtures where solids with different shapes and thermal characteristics are dispersed in the liquid phase.

In this paper, samples of commercial fruit salad (composed of five different fruits with various geometries and thermal properties) were canned in glass jars and submitted to heat treatment.

The objectives of this work were (i) to study the temperature distribution and the thermal behaviour of both fruit pieces and

syrup during the process and (ii) to develop and experimentally validate a computational fluid dynamics (CFD) model of the process itself.

## 2. Materials and methods

### 2.1. Plant and process details

The thermal treatment of fruit salad and sugar syrup in glass jar was studied taking into consideration only the heating phase of the thermal process as commercial sterility is generally achieved at the end of this stage. Tests were carried out in a small scale static pasteuriser (JBT FoodTech, Parma, Italy), controlled by PLC. Inside the pasteuriser (width = 550 mm; length = 730 mm) water was sprayed over the containers from two nozzles at a rate of  $2800 \text{ l} \cdot \text{h}^{-1}$  with a spread angle of  $120^\circ$ . Hot water temperature was set at  $93^\circ\text{C}$  and samples were heated from  $22$  to  $85^\circ\text{C}$  at the slowest heating point (SHP). The water was heated and cooled through a “tube in tube” heat exchanger where the heating and cooling media were water vapour and icy water, respectively. The jar was positioned at the centre of the pasteuriser between the nozzles and was surrounded with other jars (filled with the same product) hence reproducing as better as possible the operating conditions of the actual industrial process.

During preliminary trials, no temperature variations were observed among jars placed in various positions of the plant and also along the circumference of a single jar. This was due to the high water flow and to the nozzles with high spreads angle, allowing homogeneous temperature distribution inside the pasteurizer.

Three repeated thermal treatments were performed on three different jars in order to evaluate the average temperatures and standard deviations of syrup and fruit pieces, as described below (Section 2.3). The overall coefficient of variation (standard

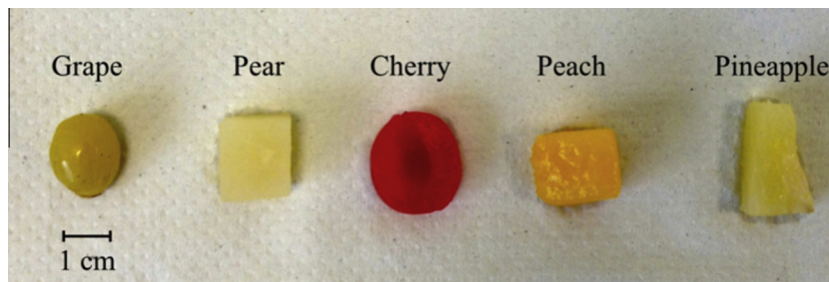


Fig. 1. Visual comparison of the different kinds of fruits used in the experiments.

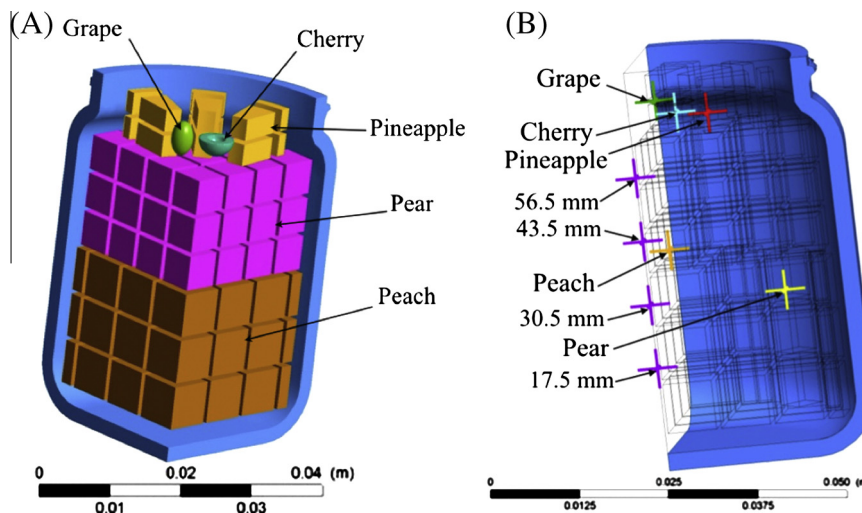


Fig. 2. 3D model of the distribution of the fruits inside the jar (panel A) and thermocouple location (panel B).

deviation/average temperature \* 100), both for syrup and fruit pieces resulted lower than 5% and hence, for a clear reading, in figures only average values (without error bars) are reported.

## 2.2. Sample characteristics

The fruit salad was composed of five different fruits (percentage expressed by weight): peach (52%), pear (38%), pineapple (5%), grape (3%) and cherry (2%). The pH value and the water activity of syrup and fruit mixture were measured at 25 °C. pH value resulted  $3.79 \pm 0.05$ , and it was obtained with a pH meter (Jenway, Staffordshire, UK), previously calibrated with standard solutions at pH = 4.02 and 7.00. Water activity value ( $a_w$ ) was  $0.988 \pm 0.005$  and it was determined with an Aqualab 4TE (Decagon Devices, Inc., WA, USA), previously calibrated with saturated salt solutions of  $MgNO_3$  ( $a_w = 0.543 \pm 0.007$ ), NaCl ( $a_w = 0.754 \pm 0.006$ ) and bi-distilled water ( $a_w = 0.999 \pm 0.001$ ) at a constant temperature of 25 °C.

Peach and pear were cubic with sides of 10 and 8 mm, respectively. Pineapple had truncated pyramid geometry (such as a titbit, with a thickness of 5 mm and major edge of 10 mm). Cherry had a hemispherical geometry with a radius of 8 mm, with a spherical hole at the centre (due to destoning) with a radius of 4 mm. The grape had an ellipsoidal geometry, with major and minor axis of 8 and 5 mm, respectively (Fig. 1). The fruits were inserted into the jar simulating an industrial filling process in the order peach, pear, pineapple, grape and cherry. The jar was then filled with 16.7% (w/w) sucrose solution measured with an electronic refractometer (Sinotech, Fujian, China). The solid/liquid ratio was 61:39 (w/w), the same as those of commercial samples. The jar used for the trials had a filling volume of 372 ml, diameter = 86.0 mm; height = 90.5 mm. Glass thickness was measured with a calliper at different locations on the side and bottom surfaces of the container and resulted in an average value of 3.5 mm. Prior to experiments, the jar was hermetically closed with a screw metal cap with a diameter of 86 mm.

## 2.3. Data acquisition

The temperatures inside the jar were measured using thermocouples (K-type; Ni/Al–Ni/Cr) connected to a multimeter acquisition system (Yokogawa Electric Corporation, Tokyo, Japan). A stainless steel multipoint temperature probe was positioned along the central axis of the jar through a hole made in the centre of the cap. This multipoint probe (length = 97.5 mm; diameter = 3.5 mm) included four thermocouples spaced every 13 mm from the tip of the probe in order to record the syrup temperature at four different

heights (17.5, 30.5, 43.5 and 56.5 mm) from the bottom of the jar. The temperature of fruit pieces was obtained by using five wire thermocouples (diameter = 0.9 mm, Gauge number = 20) inserted at the core of each fruit (Fig. 2, panel B). The temperature at half the height of the outer wall of the jar was also measured by sticking a thermocouple on the external surface with a 1 cm<sup>2</sup> of an appropriate scotch tape. Data obtained from the external wall of jars were used as temperature values for boundary conditions of the model. Both for multipoint probe and single thermocouples, an acquisition rate of 2 s was used and time–temperature data were collected in an Excel<sup>®</sup> ASCII worksheet.

## 3. CFD modelling

### 3.1. Geometry of fruit salad in the glass jar

The process of thermal treatment of fruit salad in a glass jar was simulated by means of a multidimensional CFD (computational fluid dynamic) model. The observed spatial placement of the fruit salad inside the container was replicated in a 3D CAD model. In order to reduce the computational effort required by the solution of the CFD model, the spatial domain was assumed to be symmetric with regard to two perpendicular planes through the vertical axis of the jar, hence only a quarter of the jar needed to be simulated.

The fruit pieces were spatially arranged on a regular grid (8 rows evenly distributed over the full jar height), and the spacing carefully chosen in order to obtain a solid/liquid content ratio as close as possible to that measured in the experimental tests. The resulting spatial arrangement of the fruit pieces in the model of the jar is depicted in Fig. 2 panel A.

The model geometry was then imported into the ICEM CFD<sup>®</sup> software (Canonsburg, Pennsylvania, USA) and discretized into an unstructured tetrahedral mesh. The maximum element dimension was chosen taking into consideration the domain (solid, fluid and glass). The values of maximum element edge dimension for the different fruit pieces inside the jar, together with syrup and glass are reported in Table 1.

Following the approach used by Kiziktas et al. (2010) and Dimou and Yanniotis (2011), in order to reduce the complexity of multiphase fluid calculation, the headspace was not considered in the simulation assuming the jar completely filled with product.

In order to accurately calculate the flow field near the wall of the jar, six layers of flat prismatic wedge element were used for the discretization of the fluid domain. The optimal number of wall boundary layers needed to obtain an appropriate level of accuracy

**Table 1**

Thermal properties, rheological characteristic and maximum element edge dimension for all the different kinds of fruit, together with syrup and glass.

Food	$\rho$ (kg/m <sup>3</sup> )	$\mu$ (Pa s)	$C_p$ (J/kg K)	$k$ (W/m K)	$\alpha$ (m <sup>2</sup> /s)	Max edge length <sup>g</sup> (mm)
Syrup (16.7% sugar)	1074 <sup>g</sup>	0.0258–0.00023 * T <sup>g</sup>	–	–	–	0.50
Peach	930 <sup>a</sup>	–	3700 <sup>a</sup>	0.581 <sup>b</sup>	$1.69 * 10^{-7}$	1.70
Pear	1000 <sup>b</sup>	–	3800 <sup>c</sup>	0.595 <sup>b</sup>	$1.57 * 10^{-7}$	1.50
Pineapple	1010 <sup>d</sup>	–	3490 <sup>d</sup>	0.549 <sup>d</sup>	$1.56 * 10^{-7}$	0.80
Grape	1320 <sup>e</sup>	–	3325 <sup>e</sup>	0.273 <sup>e</sup>	$0.69 * 10^{-7}$	0.45
Cherry	1049 <sup>b</sup>	–	3730 <sup>c</sup>	0.511 <sup>c</sup>	$1.31 * 10^{-7}$	0.26
Glass	2500 <sup>f</sup>	–	750 <sup>f</sup>	1.400 <sup>f</sup>	–	2.00

<sup>a</sup> Whitelock et al. (1999).

<sup>b</sup> Rahman (2008).

<sup>c</sup> ASHRAE (2006), Handbook-refrigeration.

<sup>d</sup> Padmavati and Anandharamakrishnan (2013).

<sup>e</sup> Akhijahani and Khodaei (2013).

<sup>f</sup> Incropera et al. (2006).

<sup>g</sup> Experimental value.

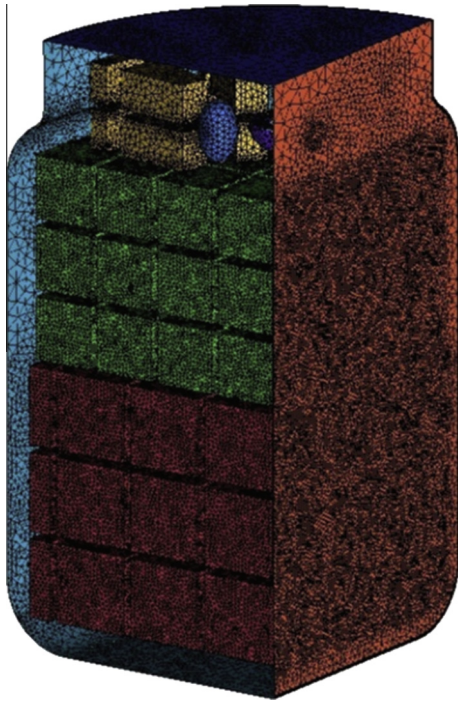


Fig. 3. 3D model of the fruits inside the jar with the mesh element.

was identified by means of a layer-independence analysis, which suggested a value for the dimension of the first element near the wall equal to 0.04 mm with a height ratio of 1.2 between layers. The final mesh with solid and fluid elements consists of  $3 \times 10^6$  elements (Fig. 3).

3.2. Numerical model

The evaluation of the field of fluid flow and thermal exchange occurring in the considered domain due to natural convection required numerical solution of the generalized transport equations:

(a) Continuity equation

$$\frac{\partial \rho}{\partial t} + \nabla \cdot (\rho V) = 0 \tag{1}$$

(b) Momentum equation

$$\frac{\partial \rho V}{\partial t} + \nabla \cdot (\rho V \cdot V) = \nabla \cdot (-p\delta + \mu(\nabla V + (\nabla V)^t)) + S_M \tag{2}$$

(c) Energy equation

$$\frac{\partial \rho h_{total}}{\partial t} - \frac{Dp}{Dt} + \nabla \cdot (\rho V h_{total}) = \nabla \cdot (k\Delta T) + S_E \tag{3}$$

where  $t$  is the time,  $V$  is the velocity vector,  $\rho$  is the density,  $p$  is the pressure,  $\mu$  is dynamic viscosity,  $k$  is thermal conductivity,  $h_{total}$  is the specific total enthalpy.

The software Ansys® CFX 14.5 (Canonsburg, Pennsylvania, USA) was chosen for the calculation. Natural convection was modelled using the Boussinesq approximation, which uses a constant density fluid model, but applies a local body gravitational force throughout the fluid that is a linear function of thermal expansivity  $\beta$  and of the local temperature difference. The buoyancy source is added to the momentum equation as follows:

$$S_M = -\rho_{ref}\beta(T - T_{ref}) \tag{4}$$

where  $\rho_{ref}$  and  $T_{ref}$  are the density and temperature at the boundary wall condition and  $g$  is the gravitational force.

No internal energy source terms ( $S_E$ ) were taken into account.

3.3. Boundary conditions

A uniform time varying temperature condition was applied to all the external surfaces of the jar and corresponded to that measured in the experimental tests. The value of initial temperature of fruit and syrup was 22 °C, while the variation of the outer wall temperature with time during the heat treatment is showed in Fig. 4 (black dotted line).

Transition in a free convection boundary layer depends both on the relative magnitude of the buoyancy and on the viscous forces in the fluid and, usually, they are correlated in terms of the Rayleigh number. For vertical plates, as glass walls, the critical Rayleigh number ( $Ra$ ) for the transition between laminar and turbulent flow is approximately  $10^9$  (Incropera et al., 2006); since the maximum  $Ra$  estimated using the maximum temperature difference and the maximum viscosity remained lower than  $10^6$  during the whole thermal treatment, laminar flow was adopted for all the simulations. The  $Ra$  value was calculated by the following equation:

$$Ra = \frac{g\beta(T_s - T_\infty)x^3}{\nu\alpha} \tag{5}$$

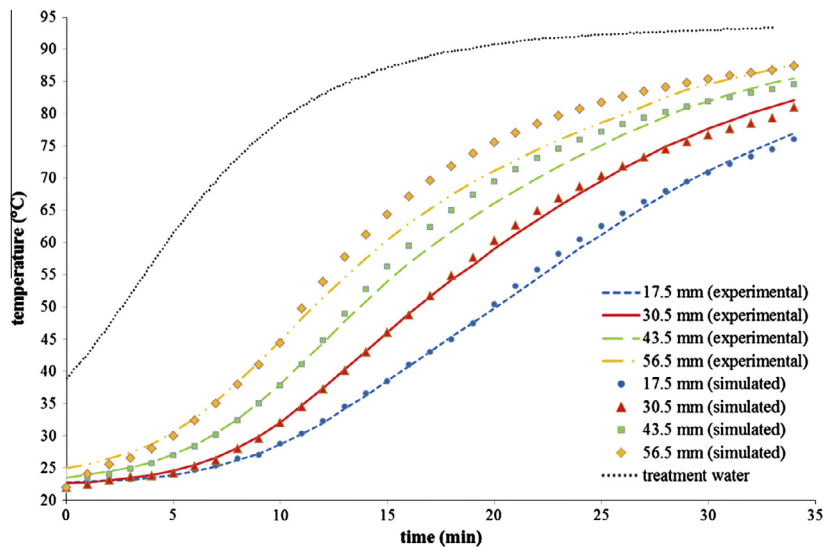


Fig. 4. Comparison of temperature profile in syrup between experimental test and mathematical model (RSD < 5%).



where  $g = 9.81$  (m/s<sup>2</sup>),  $x = 0.087$  (m) height of jar,  $T_s - T_\infty = 71$  (K) maximum temperature difference inside the jar,  $\nu = 7.9 \times 10^{-4}$  (m<sup>2</sup>/s) kinematic viscosity,  $\beta = 2.57 \times 10^{-4}$  (K<sup>-1</sup>) volumetric thermal expansion coefficient,  $\alpha = 1.56 \times 10^{-7}$  (m<sup>2</sup>/s) thermal diffusivity.

An adaptive time step option was used in order to maintain the Courant number low enough in order to accurately solve the transient heating phase. A good accuracy can be reached setting the maximum Courant number value lower of 1 (Boz et al., 2014); as a consequence a maximum time step of 0.5 s has been reached during the calculation. High resolution advection schemes were adopted for all simulations, in order to achieve second order accuracy. The convergence criterion was defined as residual root mean square (RMS) value lower than  $10^4$ .

### 3.4. Thermal and physical properties

Values of thermal and physical properties such as density ( $\rho$ ), viscosity ( $\mu$ ), specific heat ( $C_p$ ) and thermal conductivity ( $k$ ) of fruits, syrup and glass were needed for the definition of the model and the values used are summarized in Table 1. The viscosity of the

syrup was assumed to be a function of temperature and a linear interpolation from experimental data was used. By means of properties data also the thermal diffusivity ( $\alpha$ ) of each fruit was calculated by means of

$$\alpha = \frac{k}{\sigma * C_p} \quad (6)$$

and reported in Table 1.

### 3.5. Model validation

The developed model was validated by comparing experimental temperature measurements at specific points inside the glass jar with predicted ones. The accuracy of the model prediction was assessed by determining root mean square error (RMSE) and lethality ( $F_{Ts}^z$ ). The equation for RMSE determination can be expressed as:

$$RMSE = \sqrt{\frac{\sum_{n=1}^n (T_E - T_P)^2}{N}} \quad (7)$$

**Table 2**  
Validation results (RSD < 5%).

Point of measurement	RMSE	$F_{90}^{12.9}$ (min)		
		Experimental	Simulated	$\Delta F_{90}^{12.9}$
Syrup	17.5 mm	0.68	0.40	0.04
	30.5 mm	0.79	1.19	0.18
	43.5 mm	1.77	2.52	0.03
	56.5 mm	2.65	4.04	0.95
	Average	1.47		0.30
Peach	1.14	5.41	5.30	0.11
Pear	2.31	1.56	1.63	0.07
Pineapple	1.78	5.03	5.13	0.10
Grape	1.61	9.70	9.68	0.02
Cherry	1.31	7.27	7.31	0.04
Average	1.63			0.07

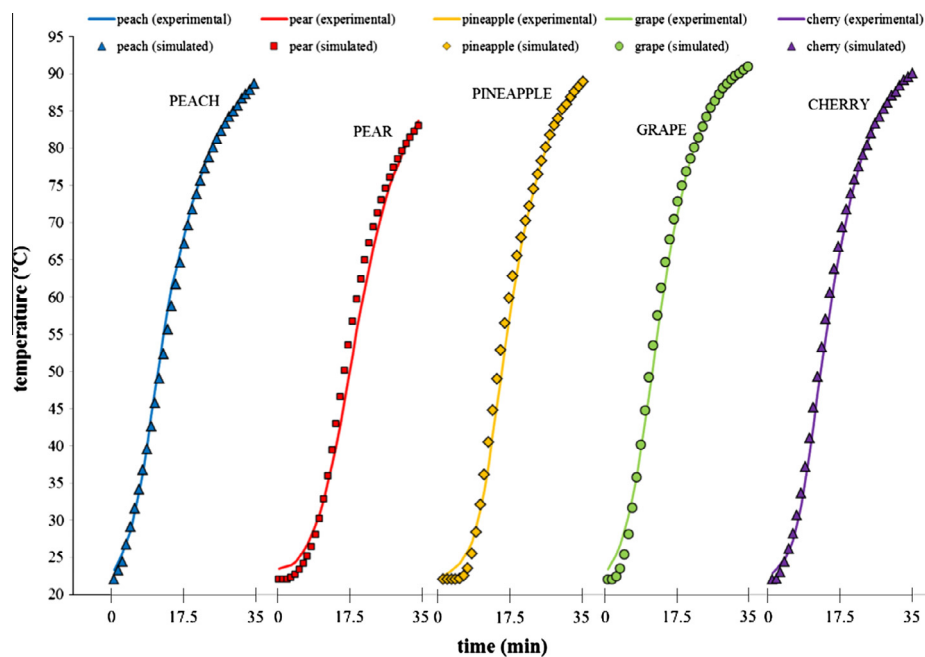


**Fig. 5.** Comparison of the temperature profile in fruit pieces between experimental test and mathematical model (RSD < 5%).

where  $T_p$  is simulated temperature and  $T_E$  is measured temperature, at time  $t$ . The effect of heat treatment and time with respect to the survival of a microorganism can be quantified by the following  $F_{Ts}^z$  value equation (Holdsworth and Simpson, 2007):

$$F_{Ts}^z = \int_0^t 10^{(T-T_{ref}/z)} dt \quad (8)$$

Lethality was calculated as an equivalent heating time at a constant temperature ( $T_{ref}$ ) of 90 °C and a  $z$  value of 12.9 °C as characteristic for *Alicyclobacillus acidoterrestris* as suggested by Silva and Gibbs (2004) for high acidity shelf stable fruit products.

## 4. Results and discussion

### 4.1. Validation results

The simulation results were in agreement with the experimental data for both the syrup and the fruits, as shown in Table 2, where validation parameters at each measurement point are reported (4 and 5 points for syrup and fruits, respectively). No significant differences were observed between experimental and simulated  $F$  values, confirming the accuracy and the reliability of the developed mathematical model. In addition, in Figs. 4 and 5 temperature profiles of the experimental and simulation treatment for syrup and fruit pieces are compared, respectively. The variations in the results of the model may be due to the distribution of the fruit pieces inside the container, the combined effects of the experimental and model assumptions such as Boussinesq approximation and the thermal properties of the materials. Furthermore, during the experiments, the location of the temperature

sensor may change the liquid flow pattern and, hence, affects the temperature profile of the sugar solution. In the simulation, small-scale instabilities were produced by the buoyancy effect. The buoyancy-produced structures might have directly interacted and coupled with the existing local turbulence and laminar modelling could not successfully predict this effect with little deviations between experimental and simulated data.

### 4.2. Slowest heating point (SHP) and temperature profile

The identification of the slowest heating point (SHP) inside the container was considered of basic importance for the effectiveness of thermal processing of our samples. The temperature distribution inside the jar was then measured at different time steps in order to describe the convective movement of the SHP.

When a fluid is subjected to a rapid temperature increase adjacent to a solid wall, part of the fluid in the wall neighbourhood expands resulting in an increase in the local pressure with significant effects in heat transfer due to thermal buoyancy effects in a gravitational force field (Aktas and Farouk, 2003). In a similar way, during thermal processing of solid–liquid mixtures, such as canned fruit salad, syrup closer to the can walls receives the heat (undergoes heat flux) thus resulting in volume expansion and density decrease while the syrup far from the walls is still at lower temperature. This phenomenon leads to development of an upward buoyancy force with a motion due to density differences. This movement also carries the colder fluid upward by viscous drag. The fluid flowing upward is deflected by the top surface of the can and starts moving in a radial direction and, by becoming heavier, starts to move downwards through the stack of fruits.

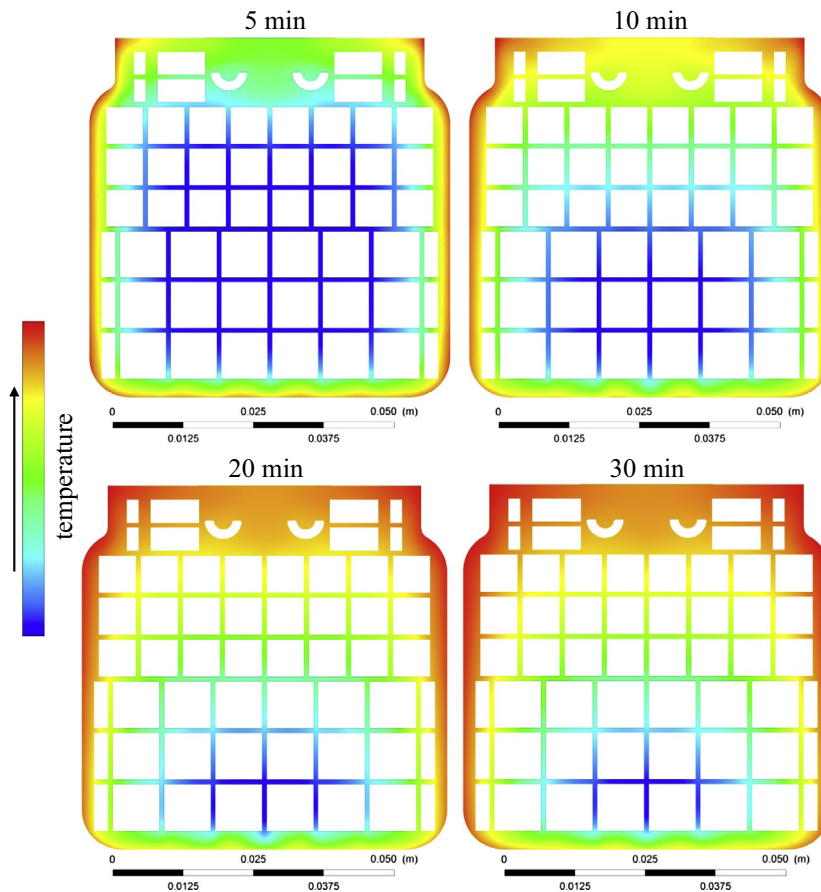


Fig. 6. Temperature distribution of the syrup at 4 different time steps (from mathematical model).

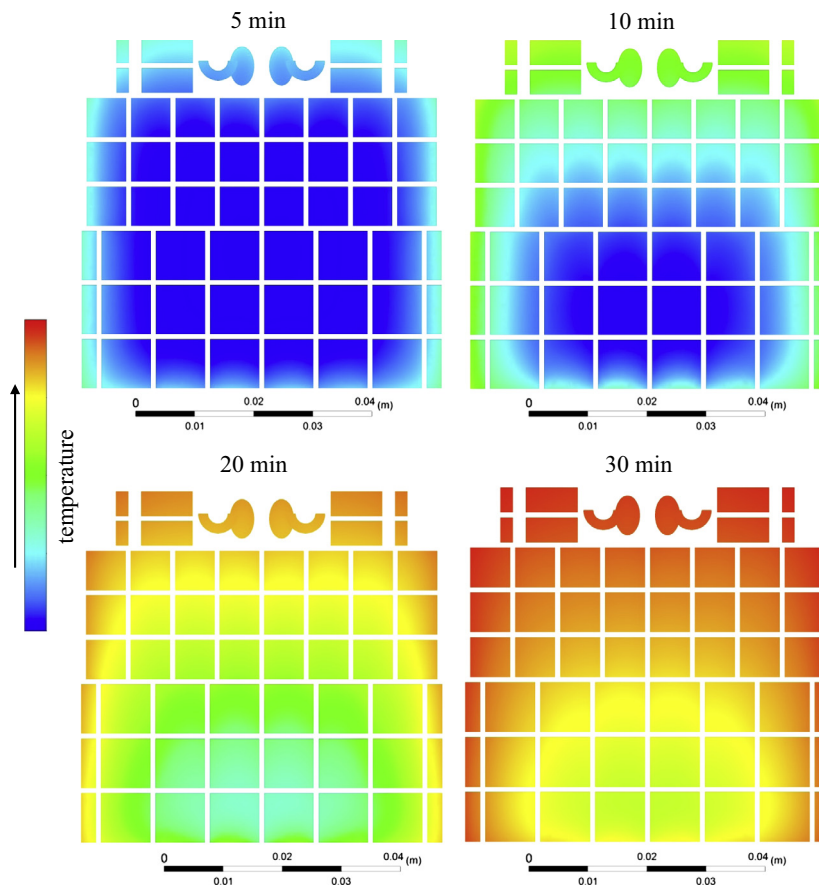


Fig. 7. Temperature distribution of the fruit pieces at 4 difference time steps (from mathematical model).

Consequently, its temperature decreases as it comes in contact with colder pieces of fruits and syrup, and a new cycle starts from the bottom. These convective movements create a recirculating flow thus increasing the rate of heat transfer. This observation is similar to the results obtained by other Authors for natural convection heating mechanism (Ghani et al., 1999; Padmavati and Anandharamakrishnan, 2013). The maximum value of liquid velocity was observed close to the wall of the jar (due to the higher temperature gradient between the jar wall and the thin liquid layer close to the wall). When solid and impermeable particles were distributed into the fluid, the velocity profile changed due to the heat exchange and surface deflections: the flow was very slow through the stack of solid particles in the horizontal direction while on the contrary it showed an increase between solids in the vertical direction.

In the case of pure convection heating of liquids, the slowest heating point (SHP) is located at about 10–15% of the can height (Padmavati and Anandharamakrishnan, 2013), but in the case of solid–liquid food mixtures heated by a combination of conduction and convection, SHP location is more complex to determine. Under our experimental conditions, the SHP of the canned fruit salad was not at the geometric centre of the can or at a can height of 10–15% but at an intermediate position between these (19–20% of the can height). The position of SHP is well shown by the  $F$  value of the various fruits: pear pieces presented the lowest  $F$  value because this kind of fruit was positioned closer to the SHP.

The natural convection effects also influenced the heating of the fruit pieces. As shown in Table 2, the fruits positioned close to the top of the jar showed a simulated  $F$  value higher than those placed close to the bottom: grape = 9.68 min, peach = 5.30 min.

When there is a marked effect of natural convection heating, thermal stratification takes place (observation based on the fluid movement due to buoyancy effects explained above). Fig. 6 shows temperature stratification for the syrup during heating phase, at 4 different time steps (5, 10, 20 and 30 min), while Fig. 7 reports the temperature stratification along the fruit pieces at the same time steps (both figures come from the graphical representation of the mathematical model).

## 5. Conclusions

In this study, a 3D CFD model was developed in order to predict the temperature profiles, to identify the slowest heating point (SHP) and to describe the flow field during the pasteurization process of a fruit salad composed of five kinds of fruit canned in a glass jar and filled with 16.7% sugar syrup.

Calculated experimental  $F_{90}^{12.9}$  values resulted different between the various fruits and, in particular, they were a function of position, characteristic dimensions and thermal properties; moreover, experimental  $F$  values were also greatly influenced by the natural convection motion of the syrup. Pear pieces showed the lowest pasteurizing value while grape the highest one: the first presented a high characteristic dimension (4 mm) and was positioned near the SHP while the latter's second had a lowest dimension (2.5 mm) and was positioned at the top of the jar where syrup presented the highest temperature.

Concerning the proposed CFD model, an appreciable agreement, expressed as RMSE, between simulated and experimental values of temperature both for syrup (1.47 °C) and fruit pieces (1.63 °C) was obtained: the model can be thus considered successfully validated

and applicable for the simulation and prediction of thermal processes of canned fruit salad.

Finally, an increase in the reliability of the model by minimizing the differences with experimental data could be achieved by enhancing temperature measurements inside syrup and fruits with reference to position inside the jar during the thermal process.

## References

- Akhijahani, H.S., Khodaei, J., 2013. Investigation of specific heat and thermal conductivity of rassa grape (*Vitis vinifera* L.) as a function of moisture content. *World Appl. Sci. J.* 22, 939–947.
- Aktas, M.K., Farouk, B., 2003. Numerical simulation of developing natural convection in an enclosure due to rapid heating. *Int. J. Heat Mass Trans.* 46, 2253–2261.
- Anandharamakrishnan, C., 2011. Applications of computational fluid dynamics in food processing operations. In: Murphy, A.D. (Ed.), *Computational Fluid Dynamics: Theory, Analysis and Applications*. Nova Publishers, New York, pp. 297–316 (Chapter 9).
- ASHRAE, (2006). *Thermal Properties of Foods. Handbook Refrigeration (Chapter 9)*.
- Boz, Z., Erdogdu, F., Tutar, M., 2014. Effects of mesh refinement, time step size and numerical scheme on the computational modeling of temperature evolution during natural-convection heating. *J. Food Eng.* 123, 8–16.
- Chen, C.R., Ramaswamy, H.S., 2007. Visual basic computer simulation package for thermal process calculations. *Chem. Eng. Process.* 46, 603–613.
- Chhanwal, N., Tank, A., Raghavarao, K.S.M.S., Anandharamakrishnan, C., 2012. Computational fluid dynamics applications in bread baking process. *Food Bioprocess Technol.* 5, 1157–1172.
- Dimou, A., Yanniotis, S., 2011. 3D numerical simulation of asparagus sterilization in a still can using computational fluid dynamics. *J. Food Eng.* 104, 394–403.
- Ghani, A.G., Farid, M.M., 2006. Using the computational fluid dynamics to analyse the thermal sterilization of solid–liquid food mixture in cans. *Innovative Food Sci. Emerg. Technol.* 7, 55–61.
- Ghani, A.G., Farid, M.M., Chen, X.D., 2002. Numerical simulation of transient temperature and velocity profiles in a horizontal can during sterilization using computational fluid dynamics. *J. Food Eng.* 51, 77–83.
- Ghani, A.G., Farid, M.M., Chen, X.D., Richards, P., 1999. Numerical simulation of natural convection heating of canned food by computational fluid dynamics. *J. Food Eng.* 41, 55–64.
- Holdsworth, D., Simpson, R., 2007. *Thermal Processing of Packaged Foods, Food Engineering Series*. Springer, New York.
- Incropera, F.P., DeWitt, D.P., Bergman, T.L., Lavine, A.S., 2006. *Fundamental of Heat and Mass Transfer*. John Wiley & Sons.
- Kiziktas, S., Erdogdu, F., Palazoglu, T.K., 2010. Simulation of heat transfer for solid–liquid food mixtures in cans and model validation under pasteurization conditions. *J. Food Eng.* 97, 449–456.
- Kumar, A., Bhattacharya, M., Blaylock, J., 1990. Numerical simulation of natural convection heating of canned thick viscous liquid food products. *J. Food Sci.* 55, 1403–1411.
- Kuriakose, R., Anandharamakrishnan, C., 2010. Computational fluid dynamics (CFD) applications in spray drying of food products. *Trends Food Sci. Technol.* 21, 383–398.
- Padmavati, R., Anandharamakrishnan, C., 2013. Computational fluid dynamics modeling of the thermal processing of canned pineapple slices and titbits. *Food Bioprocess Technol.* 6, 882–895.
- Rabiey, L., Flick, D., Duquenoy, A., 2007. 3D simulations of heat transfer and liquid flow during sterilization of large particles in a cylindrical vertical can. *J. Food Eng.* 82, 409–417.
- Rahman, M.S., 2008. *Food Properties Handbook*. CRC, Boca Raton.
- Silva, F.V., Gibbs, P., 2004. Target selection in designing pasteurization processes for shelf-stable high-acid fruit products. *Crit. Rev. Food Sci. Nutr.* 44 (5), 353–360.
- Sun, D.W., 2007. *Computational Fluid Dynamics in Food Processing*. CRC, Boca Raton.
- Varma, M.N., Kannan, A., 2005. Enhanced food sterilization through inclination of the container walls and geometry modifications. *Int. J. Heat Trans.* 48, 3753–3762.
- Weng, Z.J., 2005. Thermal processing of canned foods. In: Sun, Da-Wen (Ed.), *Thermal Food Processing – New Technologies and Quality Issues*. CRC-Taylor and Francis, Boca Raton (Chapter 11).
- Whitelock, D.P., Bruswitz, G.H., Ghajar, A.J., 1999. Thermal/physical properties affect predicted weight loss of fresh peaches. *Am. Soc. Agric. Eng.* 42, 1047–1053.
- Xia, B., Sun, D.W., 2002. Review: applications of computational fluid dynamics (CFD) in the food industry. *Comput. Electron. Agric.* 34, 5–24.